Regular Article

Effect of nanoparticle dispersion on glass transition in thin films of polymer nanocomposites

S. Chandran and J.K. Basu[a]

Department of Physics, Indian Institute of Science, Bangalore, 560012, India

Abstract. We present spectroscopic ellipsometry measurements on thin films of polymer nanocomposites consisting of gold nanoparticles embedded in poly(styrene). The temperature dependence of thickness variation is used to estimate the glass transition temperature, T_g. In these thin films we find a significant dependence of T_g on the nature of dispersion of the embedded nanoparticles. Our work thus highlights the crucial role played by the particle polymer interface morphology in determining the glass transition in particular and thermo-mechanical properties of such nanocomposite films.

1 Introduction

Polymer nanocomposites (PNC) are a novel class of materials usually consisting of inorganic nanoparticles with tunable electrical, optical and magnetic properties embedded in a polymer matrix which can be readily processed using solvent or thermal treatments [1–3]. The enormous technological potential of such materials has also led to rapid growth in fundamental investigation on the dispersion and in correlation with the ultimate physical properties attainable in such materials [1–10]. Since most of the polymer used play the role of the passive matrix and are glassy in the bulk, a large amount of work has been devoted to understand how the glass transition and glassy dynamics is affected by incorporation of nanoparticles [4,5,7,10]. This is not only helpful in understanding and and hence controlling the thermo-mechanical properties of these PNCs but also obtaining a general understanding of the much studied but controversial field of finite-size and interface effects on glass transition of polymers [5,8,10–18]. Although the equivalence of finite-size effects in bulk PNCs and polymer thin films [5,10] or polymers confined in nanopores [14] has been shown, the role of dispersion of nanoparticles in PNC films has not been adequately studied or understood [15,19]. Here, we show how the dispersion of 1-octadecanethiol (ODT)-capped gold nanoparticles (AuNP) at various densities inside thin poly(styrene) (PS) films of thickness 75 ± 3 nm is related to the glass transition temperature, T_g, of the thin films. The T_g's have been estimated from spectroscopic ellipsometry on these thin films prepared with various volume fractions, ϕ_p, of ODT-capped AuNP in PS matrix and under different conditions of thermal annealing to control their dispersion.

2 Experimental details

2.1 Synthesis

The thiol functionalized gold nanoparticles (AuNPs) were synthesized by reduction of hydrogen tetrachloroaurate trihydrate ($HAuCl_4.3H_2O$) with super hydride (lithium triehtylborohydride) in Tetrahydrofuran (THF) after stirring for 20 minutes in the presence of ODT as described earlier [20–23]. All chemicals, unless stated otherwise, were purchased from Sigma-Aldrich. After stirring the growth solution for a couple of hours, the growth is stopped by adding ethanol (Merck). The particles were cleaned for excess ODT by selective precipitation using the mixture of THF and ethanol and then centrifuging the mixture. Finally the ethanol-THF mixture was decanted and the residue was dried for 12 hours.

2.2 Characterization ODT-capped AuNPs

The size of the synthesised particles were estimated from Transmission Electron Microscopy (TEM) images, obtained using Technai G20 High Resolution TEM. The TEM micrograph in fig. 1 shows that reasonably monodisperse gold particles were obtained. Thermo gravimetric analysis (TA Instruments) is used to find the relative fraction of ODT and gold in ODT-capped AuNPs. The obtained fraction along with the size were used to estimate the grafting density σ ($= 5.5$ chains/nm^2) of ODT on the nanoparticle surface.

---
[a] e-mail: basu@physics.iisc.ernet.in
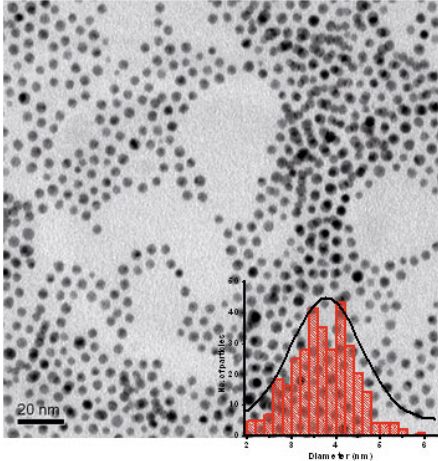
Fig. 1. Transmission electron microscopic images of ODT-capped AuNPs. Inset: histogram of the particle diameters and a Gaussian fit to show the mean particle size 3.79 nm.

Table 1. Sample identification.

Sample	Volume Fraction percentage ϕ_p	Mean interparticle distance [a] h (nm)	h/R_g
A1	0.1	50.49	6.33
A2	0.3	33.07	4.14
A3	0.5	26.89	3.37
A4	0.55	26.84	3.24
A5	0.75	22.67	2.84
A6	1.22	18.30	2.29

[a] The mean interparticle distance given here is applicable only for the annealed samples, where the particles are well dispersed in the volume [5].

2.3 Preparation of nanocomposite thin films

ODT-grafted gold nanoparticles and Poly-(styrene) ($M_w = 97400$ g/mol with a calorimetric T_g of 106 °C; radius of gyration, $R_g = 8$ nm) were dissolved separately in toluene for 12 hours. Once both were dissolved completely, they were mixed and then stirred for ~ 12 hours for ensuring a homogeneous dispersion. Highly polished silicon wafers (Vin Karola, USA) with a native silicon dioxide layer (~ 2 nm) served as substrates for ellipsometric measurements. The silicon surface is thoroughly cleaned with acidic piranha, to make the surface hydrophilic before spin coating. The films as identified in table 1 were then spin coated at a rate of 3000 rpm (for 100 s). The films were annealed at two different conditions: (a) ~ 150 °C for 12 hours, (b) ~ 70 °C for 4 hours in vacuum better than $\sim 5 \times 10^{-3}$ mbar. Annealing is done at different temperatures one below and another above the T_g of the matrix to control different dispersions of the particles and still ensuring the removal of trapped solvent.

2.4 Atomic force ficroscopy

Atomic force microscopy (AFM, NT-MDT, Russia) is used in contact mode to get the surface morphology of the samples. Cantilevers (force constant = 0.03–0.2 N/m) with a radius of curvature 10 nm were used. The images were collected at a scan frequency of 1 Hz and at a minimum set point as determined from force-distance curves, to ensure that the tip does not drag on the sample.

2.5 Ellipsometry

Temperature-dependent ellipsometry measurements were carried out at a fixed angle of incidence of 70° using a spectroscopic ellipsometer SE850 (Sentech, Germany) connected to a home-made vacuum (3×10^{-2} mbar) temperature cell. The measurements were performed in cooling at a rate of 1 °C/min starting from 150 °C (T_g of bulk PS from differential scanning calorimetry is 105 °C and that measured in thin film without nanoparticles is 106 °C). The Ψ and Δ values were collected from the highest to room temperature continuously in the cooling cycle. An effective medium layer with Maxwell-Garnett type of dispersion [24] is assumed for the sample (PNC thin film) layer for finding the complex dielectric function ϵ_f and thereby the thickness d of the film. The Maxwell-Garnett type dispersion assumes a mixture of two distinct materials, each possessing the optical properties of the bulk material, and requires that the particles dispersed in the host material do not interact with one another. This can be satisfied by keeping the volume fraction of the dispersed particles low. The complex dielectric function, ϵ_f, of the film can be written as

$$\frac{\epsilon_f - \epsilon_m}{\epsilon_f + 2\epsilon_m} = F \frac{\epsilon_p - \epsilon_m}{\epsilon_p + 2\epsilon_m}, \tag{1}$$

where ϵ_m, ϵ_p are the dielectric constants of the matrix and the particulate fillers, respectively, and F is the fill factor of the particles. The thickness d of the films was obtained by fitting Ψ and Δ with a model as specified. The obtained thickness is plotted as a function of temperature, and the respective T_g is obtained from the change in slope, as shown in fig. 3.

3 Results and discussion

The AFM images in fig. 2 shows the dramatic role of high temperature (150 °C) thermal annealing on dispersion of ODT-capped gold nanoparticles in PS thin films. The changes in morphology of low temperature (70 °C for 4 hours) annealed films (fig. 3) is less significant, in comparison, but is also dependent on volume fraction. Although it thus seems to indicate the possibility of the presence of some surface mobility even at this low temperature (as compared to the bulk T_g) along the lines of [17, 18]. The dispersion of the nanoparticles is complete when annealed above bulk T_g. The height of the nanoparticle domains visible in unannealed and 70 °C annealed films are
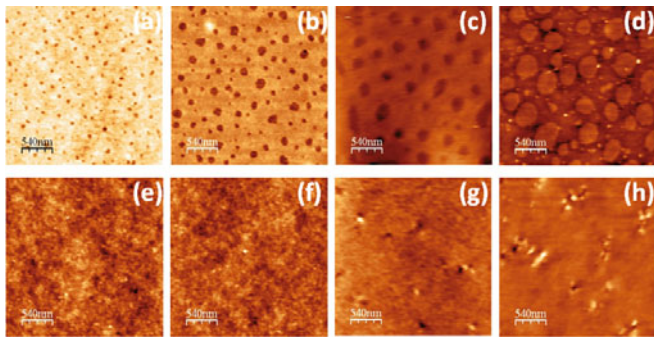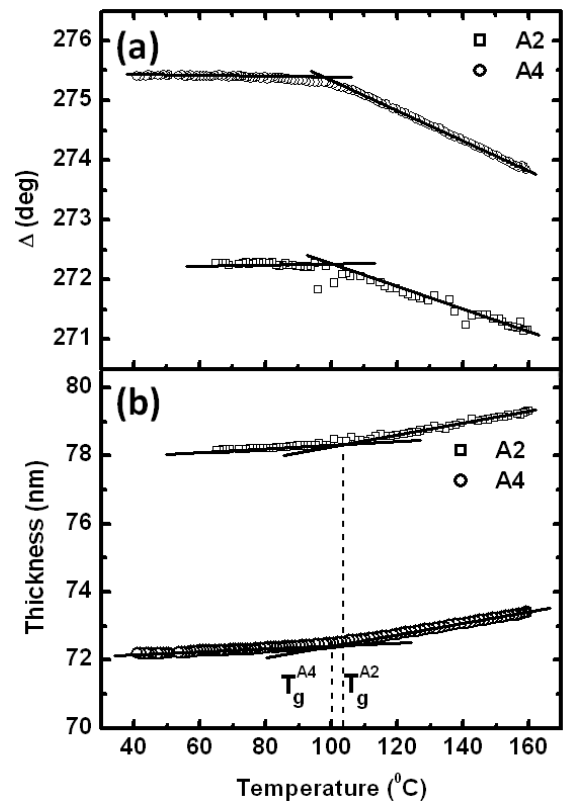
Fig. 2. AFM image showing the surface morphology of un-annealed (a,b,c,d) and annealed at 150 °C (e,f,g,h) for samples A1, A4, A5, A6, respectively.
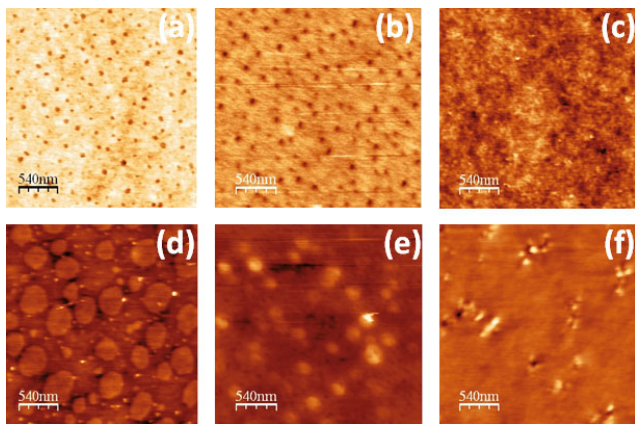
Fig. 3. AFM image showing the surface morphology of un-annealed (a,d), annealed at 70 °C (for 4 hours) (b,e) and at 150 °C (for 12 hours) (c,f) for the samples A1 and A6, respectively.

Fig. 4. (a) Δ as a function of temperature, T, at a fixed wavelength of 350 nm for samples A2 and A4 as indicated in the panel. (b) Thickness as a function of T. The continuous lines in (a) and (b) are the linear fits in the respective regions. The T_g of the respective samples is indicated in the panel.

~ 3 nm, which seems to indicate that it is a monolayer of the nanoparticles. The dispersion of nanoparticles in polymers is a great challenge [25] and the nature of dispersion depends, to a large extent, on the interaction between the nanoparticles and the host polymer. We (not presented here) and others [15, 26] have found that gold nanoparticles capped with appropriate polymers can form stable dispersions in suitable host polymer matrix even without annealing. We will discuss the role of thermal treatment and especially of the consequent degree of dispersion of nanoparticles in the polymer matrices on the glass transition behaviour of PNC films.

Several authors have reported their investigations of thermo-mechanical properties in general and glass transition in particular on polymers confined in pores [12–14] or in thin films as well as bulk and thin film polymer nanocomposites [8–11, 16, 17]. Widely varying thermal treatment have been used for thin polymer films and this has resulted in a great controversy about the finite-size effect on glass transition of such films [11, 16, 18]. The available literature on bulk [5, 7–10] and thin film PNCs [15, 19, 27, 28] is also controversial in terms of the conclusions drawn on the role of confinement and surface effects in such systems. For example, some authors

have observed large changes in T_g of thin film polymer nanocomposites as a function of ϕ_p of nanoparticles in polymers. However, in most of these cases, it turns out that the films have either not been annealed or are annealed at temperatures below the T_g of the host polymer [15]. In other cases, some authors have found small changes or no change with increasing volume fraction of nanoparticles when the films have been annealed at temperatures above the host polymer T_g [27, 28]. We have, hence used a thermal-expansivity–based study of glass transition of, otherwise identical, thin film polymer nanocomposites which have been annealed at temperatures below and above the host polymer T_g. In fig. 3, a typical variation of the spectroscopic ellipsometry parameter, Δ (at a wavelength of 350 nm) as a function of measured temperature, T, is shown for two such films which have been annealed at 150 °C. The T_g can be clearly identified. We have also analyzed the full spectroscopic ellipsometry data to extract the thickness at each temperature. Within errors, the T_g obtained from the two analyses are identical; hence for all other films we have used the variation of Δ with T to extract the respective, T_g.

The results are summarised in fig. 4 for both the low temperature and high-temperature annealed films. From fig. 4(a) we observe that for the low-temperature annealed films, at the lowest ϕ_p, T_g increases with respect to the PS
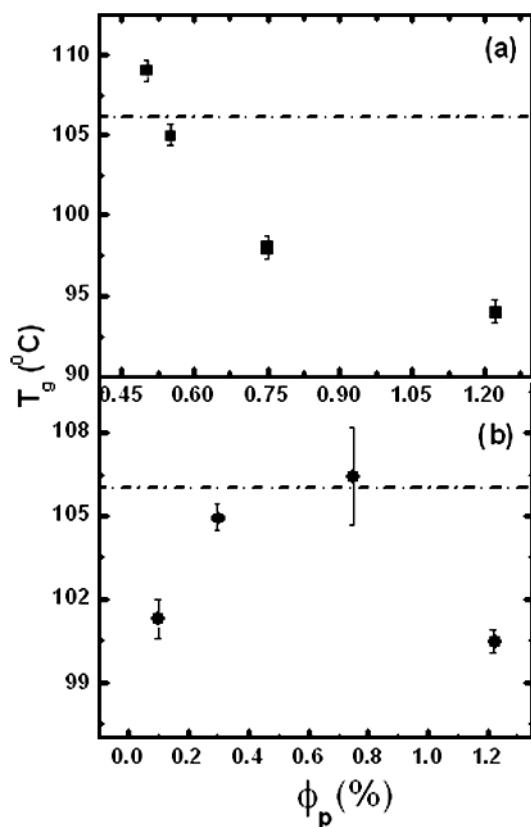
Fig. 5. Variation of T_g as a function of volume fraction percentage, ϕ_p, of the ODT-capped AuNPs after annealing at 70 °C (a) and 150 °C (b). The dot-dashed line in both panels gives the calorimetric T_g of PS.

film of identical thickness. However, with increasing ϕ_p, we observe significant depression of T_g. This is something which is quite unusual and, to our knowledge, has not been observed earlier for similar systems. It seems clear from the AFM images that there is considerable surface segregation of the nanoparticles for all the unannealed and low-temperature annealed films. Such an effect was found to lead to an enhancement of T_g in an earlier work [15]. However, the depression in T_g is not expected for our films with higher ϕ_p since the nature of the dispersion does not seem to change significantly with increasing ϕ_p. The decrease of T_g with increasing ϕ_p is due to the possible depletion of polymer chains around the large nanoparticle domains at the film surface. The variation of T_g changes quite dramatically with high-temperature annealing of the films. From fig. 4(b) we find that the T_g values are either equal to neat PS or depressed compared to it, irrespective of ϕ_p. However, the effect is not as strong as that observed for the films annealed at lower temperature. For well-dispersed ODT-capped Au NP particles in PS this would be expected, since the PS chains are expected to be depleted from the ODT interface due to unfavorable interactions leading to enhancement in segmental mobility at the nanoparticle polymer interface and hence a reduction in T_g. It might be noted here that an increase in ϕ_p corresponds to either a reduction in film thickness or pore

size for bulk polymers confined in pores. At the volume fractions investigated, the mean interparticle separation is ~ 50–100 nm. At such confinement dimensions the reduction in T_g has been found to be quite small compared to the bulk polymers [12–14, 17]. Thus the observed deviations in T_g for the PNC thin films at the studied ϕ_p is not unusual. However, our primary finding is that the extent of such variations as well as the anomalous nature of such variations, that has been observed earlier [15], is very sensitive to the nature of dispersion of nanoparticles and hence only equilibrated films which have been well annealed give the appropriate nature of variation of T_g in thin films of PNCs.

4 Conclusion

In conclusion we have shown how thermal treatment of nanoparticle-embedded polymer films can lead to significant variation in the morphology and dispersion of the nanoparticles in the host polymer. We have shown that as a consequence, the nature of variation of glass transition in such films changes dramatically due to sensitive surface and interface effects at the polymer-nanoparticle interface. Further wok involving the interplay of confinement and surface effects is underway to better understand the physics of glass transition in such systems.

References

1. R.B. Thompson, V.V. Ginzburg, M.W. Matson, C. Balazs, Science **292**, 2469 (2001).
2. S.C. Warren, L.C. Messina, L.S. Slaughter, M. Kamperman, Q. Zhou, S.M. Gruner, F.J. DiSalvo, U. Wiesner, Science **320**, 1748 (2008).
3. M.R. Bockstaller, E.L. Thomas, Phys. Rev. Lett. **93**, 166106 (2004).
4. M.K. Corbierre, N.S. Cameron, M. Sutton, K. Laaziri, R.B. Lennox, Langmuir **21**, 6063 (2005).
5. S. Srivastava, J.K. Basu, Phys. Rev. Lett. **98**, 165701 (2007).
6. F.W. Starr, T.B. Schroder, S.C. Glotzer, Phys. Rev. E **64**, 021802 (2001).
7. A. Bansal, H. Yang, C. Li, B.C. Benicewicz, S.K. Kumar, L.S. Schadler, J. Polym. Sci. Part B-Polym. Phys. **44**, 2944 (2006).
8. V. Pryamitsyn, V. Ganesan, Macromolecules **43**, 5851 (2010).
9. J.M. Kropka, V. Pryamitsyn, V. Ganesan, Phys. Rev. Lett. **101**, 075702 (2008).
10. A. Bansal, H. Yang, C. Li, K. Cho, B.C. Benicewicz, S.K. Kumar, L.S. Schadler, Nat. Mater. **4**, 693 (2005).
11. S. Napolitano, M. Wubbenhorst, Nat. Commun. **260**, 2 (2011).
12. C.L. Jackson, G.B. McKenna, J. Non-Cryst. Solids **131-133**, 221 (1991).

13. J. Zhang, G. Liu, J. Jonas, J. Phys. Chem **96**, 3478 (1992).
14. Y.P. Koh, Q. Li, S.L. Simon, Thermochim. Acta **492**, 45 (2009).
15. A. Arceo, L. Meli, P.F. Green, Nano Lett. **8**, 2271 (2008).
16. M. Tress, M. Erber, E.U. Mapesa, H. Huth, J. Muller, A. Serghei, C. Schick, K.-J. Eichhorn, B. Voit, F. Kremer, Macromolecules **43**, 9937 (2010).
17. Z. Fakhraai, J.A. Forrest, Science **319**, 600 (2008).
18. Z. Yang, Y. Fujii, F.K. Lee, C.-H. Lam, O.K.C. Tsui, Science **328**, 1676 (2010).
19. J.Q. Pham *et al.*, J. Polym. Sci. Part B-Polym. Phys. **41**, 3339 (2003).
20. M.K. Corbierre, N.S. Cameron, M. Sutton, S.G. Mochrie, L.B. Lurio, A. Ruhm, R.B. Lennox, J. Am. Chem. Soc. **123**, 10411 (2001).
21. M.K. Corbierre, N.S. Cameron, R.B. Lennox, Langmuir **20**, 2867 (2004).
22. S. Srivastava, S. Chandran, A.K. Kandar, C.K. Sarika, J.K. Basu, S. Narayanan, A. Sandy, J. Chem. Phys. **133**, 151105 (2010).
23. A.K. Kandar, S. Srivastava, J.K. Basu, M.K. Mukhopadhyay, S. Seifert, S. Narayanan, J. Chem. Phys. **130**, 121102 (2009).
24. J.C. Maxwell-Garnett, Philos. Trans. R. Soc. London, Ser. A **203**, 385 (1904).
25. M.E. Mackay, A. Tuteja, P.M. Duxbury, C.J. Hawker, B.V. Horn, Z. Guan, G. Chen, R.S. Krishnan, Science **311**, 1740 (2006).
26. X.C. Chen, P.F. Green, Langmuir **26**, 3659 (2010).
27. J.H. Xavier, S. Sharma, Y.S. Seo, R. Isseroff, T. Koga, H. White, A. Ulman, K. Shin, S.K. Satija, J. Sokolov, M.H. Rafailovich, Macromolecules **39**, 2972 (2006).
28. T. Koga, C. Li, M.K. Endoh, J. Koo, M. Rafailovich, S. Narayanan, D.R. Lee, L.B. Lurio, S.K. Sinha, Phys. Rev. Lett. **104**, 066101 (2010).